

Complex brain networks: From topological communities to clustered dynamics

LUCIA ZEMANOVÁ¹, GORKA ZAMORA-LÓPEZ¹, CHANGSONG ZHOU^{2,*}
and JÜRGEN KURTHS¹

¹Institute of Physics, University of Potsdam, 14469 Potsdam, Germany

²Department of Physics, Hong Kong Baptist University, Kowloon Tong, Hong Kong

*Corresponding author. E-mail: cszhou@hkbu.edu.hk

Abstract. Recent research has revealed a rich and complicated network topology in the cortical connectivity of mammalian brains. A challenging task is to understand the implications of such network structures on the functional organisation of the brain activities. We investigate synchronisation dynamics on the corticocortical network of the cat by modelling each node of the network (cortical area) with a subnetwork of interacting excitable neurons. We find that this network of networks displays clustered synchronisation behaviour and the dynamical clusters closely coincide with the topological community structures observed in the anatomical network. The correlation between the firing rate of the areas and the areal intensity is additionally examined. Our results provide insights into the relationship between the global organisation and the functional specialisation of the brain cortex.

Keywords. Cortical networks; multilevel model; anatomical hierarchy; functional hierarchy; clustered synchronisation.

PACS Nos 87.18.Sn; 89.75.Da; 89.75.Fb; 05.45.Xt

1. Introduction

The organisation and features of complex networks have been the centre of attention for over a decade [1]. Several types of networks have been identified based on their topological properties. In parallel, dynamics of network elements and their ability to synchronise have been intensively investigated [2]. Recent research has focused on the relationship between structure and dynamics. In neuroscience, the network analysis of the anatomical connectivity of the mammalian cortex and the functional connectivity of the human brain has shown that both types of brain networks share typical features of many other real complex networks [3]. Neural anatomical network structures at various levels, especially the large-scale cortical networks, display characteristics of small-world networks, e.g., high clustering and short path length. These properties allow the system to perform both specialised and integrated processes. The organisation of the functional connectivity based on

large-scale measurement of brain activities, such as fMRI or EEG [4], also exhibits basic properties of small-world and scale-free networks [3].

It is of fundamental importance to understand the interrelationship between the topological structures and the activity of the brain. To better comprehend the principles underlying the dynamics of the brain, various models of neuronal activity have been studied, ranging from generic oscillators to realistic neuronal models [5,6]. In the present study, the dynamics of cortical networks are simulated by a multilevel model, *a network of networks*, where each cortical area is modelled by a subnetwork of interacting excitable neurons. These networks have a typical small-world (SW) topology that captures the important features in the architecture of biological neuronal networks where most of the connections are local and a small fraction of the connections can be of a long-range character. We focus here on the systems level of the connectivity formed by long-range projections among cortical areas, which connect the SW subnetworks in our model. Our central task is to use this hierarchical neural model to study the impact of the anatomical topology on dynamical processes. The correlations between the mean activity of the areas (subnetworks) are examined and compared to the underlying anatomical network to understand the relationship between them. Additionally, we examine the role of the node intensity (total afferent connections of an area) in the dynamics of individual areas.

2. Hierarchical model

The system we have built – a network of networks – represents a simplified anatomical structure of the brain (figure 1a). In this two-level hierarchical network, the higher (macroscopic) level corresponds to the cortical network of interconnected areas ($m = 53$) in the cat brain. The corticocortical connectivity data of the cat was collated by Scannell *et al* [7] and organised into four topological communities – visual (V), auditory (A), somato-motor (SM) and fronto-limbic (FL) (indicated by the solid lines in figure 1b) [7,8]. The lower (mesoscopic) level, representing a single cortical area, is modelled by a SW network of neurons. Such topology accounts for the basic properties of realistic neuronal connectivity at the cellular level.

Thus, in our model a single neuron represents the basic element of the hierarchical network and its dynamics are modelled as

$$\begin{aligned} \epsilon \dot{x}_{I,i} = & f(x_{I,i}) + \frac{g_{\text{int}}}{k_a} \sum_j^n M_I^L(i,j)(x_{I,j} - x_{I,i}) \\ & + \frac{g_{\text{ext}}}{\langle w \rangle} \sum_J^m M^C(I,J)L_{I,J}(i)(\bar{x}_J - x_{I,i}), \end{aligned} \quad (1)$$

$$\dot{y}_{I,i} = x_{I,i} + a_{I,i} + D\xi_{I,i}(t). \quad (2)$$

$x_{I,i}$ is a membrane potential of neuron i from area I modelled by a function $f(x_{I,i}) = x_{I,i} - \frac{x_{I,i}^3}{3} - y_{I,i}$, known as a FitzHugh–Nagumo model (FHN) (here we adopt the version from [9]). We set a time-scale parameter $\epsilon = 0.01$ and a bifurcation parameter $a_i \in (1.05, 1.15)$, where the neurons are in the excitable regime. A

weak Gaussian white noise ξ with intensity $D = 0.03$ is added (eq. (2)) to simulate natural perturbations that generate an irregular Poisson-like spiking activity of a neuron. The whole model represents resting state without particular sensory input.

The dynamics of the neurons are modulated by the input from the local small-world network ($M_I^L(i, j): i, j = 1, \dots, n$) and input from remote neurons in other areas, coupled through the cat cortex connectivity ($M^C(I, J): I, J = 1, \dots, m$). We set up that the connected areas communicate through their mean field activity $\bar{x}_I = 1/n \sum_j^n x_{I,j}$. The label $L_{I,J}(i)$ is 1 if neuron i is among the 5% within area I receiving the mean field signal from area J , otherwise, $L_{I,J}(i)$ is 0 [10]. Here, g , the coupling strength, is the main control parameter of the system dynamics, where the internal coupling g_{int} is normalised by k_a , the average number of local links in the SW subnetworks, and the external one g_{ext} by the averaged weight w of inter-areal connections.

In numerical simulations, we consider $n = 200$ neurons in each SW subnetwork, obtained by rewiring a regular array (each node connected to $k_a = 12$ nearest neighbours) by a probability of rewiring $p_{\text{rew}} = 0.3$; 25% of the local connections are inhibitory. The model (eqs (1), (2)) is simulated up to time $t = 2000$, with time step $\Delta t = 0.001$. All details of coupling properties and parameter settings can be found in [11].

3. Dynamical regimes of the model system

We explore the parameter space for g_{int} and g_{ext} and investigate how the dynamics of individual areas become synchronised due to the coupling.

In the local SWNs, the spiking dynamics and the synchronisation of the neurons are mainly controlled by the internal coupling g_{int} that determines the mutual excitation between any pair of neurons. For small g_{int} , a neuron is primarily activated by

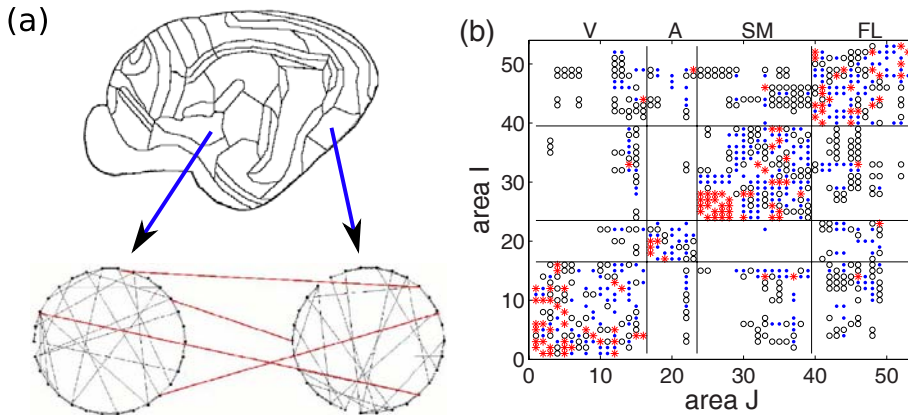


Figure 1. (a) Hierarchical model of cat brain – macroscopic level (cat cortex) and mesoscopic level (SW network). (b) Inter-areal connections in the cat cortex. The different symbols represent different connection weights: 1 (○ sparse), 2 (● intermediate) and 3 (* dense).

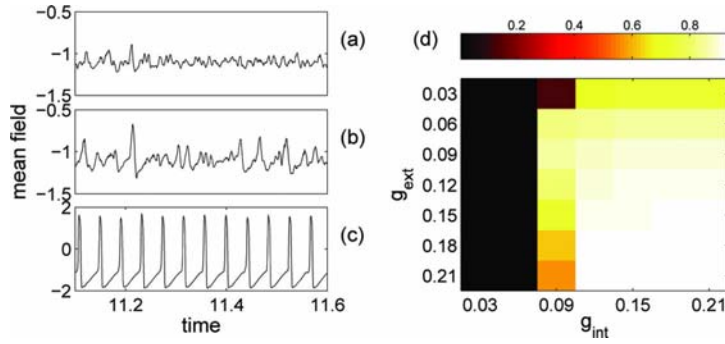


Figure 2. Time course of mean field signal of one area (\bar{x}_I) at three different couplings ($g_{\text{ext}} = g_{\text{int}}$): (a) 0.07, (b) 0.082 and (c) 0.12. (d) Dependence of the correlation R on the internal coupling strength g_{int} and external coupling strength g_{ext} .

the noise and not usually by the spiking activity of its neighbours. Thus, we observe irregular spiking patterns for individual neurons. The mean field \bar{x} is characterised by some clear deviations from the baseline, demonstrating the weak synchronisation within and also between the subnetworks (figure 2a). Such mean field activity of individual areas can be regarded as an analogue of EEG signals [12]. The weak synchronisation between the signals of the different areas is also shown by a small average correlation coefficient r (figure 3a). Increase of the coupling strength g_{int} leads to the increase of the synchronisation between the neurons within the local subnetworks, manifested by the presence of some apparent peaks in \bar{x} (figure 2b). With large enough g_{int} , the neurons are mutually excited, achieving both strongly synchronised and regular spiking behaviour (figure 2c), indicating an almost global synchronisation of the network, e.g., as observed in epilepsy [13].

To evaluate the degree of synchronisation among the mean field activities \bar{x}_I of the areas and also of the whole network, the Pearson correlation coefficient r and the average correlation coefficient R are computed as

$$r(I, J) = \frac{\langle \bar{x}_I \bar{x}_J \rangle - \langle \bar{x}_I \rangle \langle \bar{x}_J \rangle}{\sigma(\bar{x}_I) \sigma(\bar{x}_J)} \quad \text{and} \quad R = \frac{1}{m(m-1)} \sum_{I \neq J} r(I, J), \quad (3)$$

where $\langle \cdot \rangle$ denotes averaging over time.

We have averaged the results over 10 realisations of different initial conditions and the topology of the SW subnetworks for each set of the parameters. Figure 2d shows how the synchronisation depends on both the coupling strengths. As already discussed, an increase of the coupling strengths g_{int} triggers stronger interaction of the neurons and leads to a rapid growth of their synchronous activity within and across areas for non-vanishing g_{ext} . Later we keep $g_{\text{ext}} = g_{\text{int}}$ for simplicity and refer to it as g .

The patterns of the correlation matrix $r(I, J)$ for the three main dynamical regimes are shown in figure 3. Although the average levels of synchronisation R are very different, the correlation patterns display some dynamical clusters in all the cases. Here, a *dynamical (functional) cluster* is defined as a group of brain areas

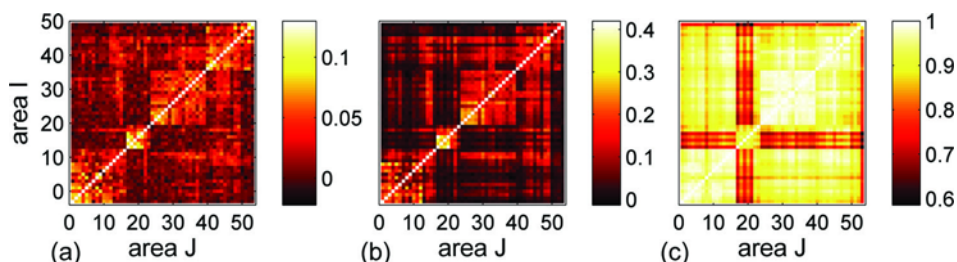


Figure 3. Correlation patterns for three different synchronisation regimes: (a) $g = 0.07$, (b) $g = 0.082$ and (c) $g = 0.12$.

communicating much more strongly within this set than with the areas in the rest of the brain [3]. In the weak synchronisation regime, e.g., $g = 0.07$ and $r \in [0, 0.13]$, four dynamical clusters are visible that resemble the underlying anatomical structure (figure 3a). The transient regime, e.g., for $g = 0.082$ and $r \in [0, 0.4]$, displays similar organisation of areas into clusters as in the weak synchronisation regime (figure 3b), but further analysis reveals that there are three major dynamical clusters (see [11]). Finally, in the strong synchronisation regime, e.g., $g = 0.12$ and $r \in [0.6, 1.0]$, we observe only two dominant clusters (figure 3c).

4. Dynamical clusters of cortical network

Using the correlation matrix, the dynamical patterns are decomposed into the four clusters in order to examine how the present dynamical clusters are related to the natural anatomical division into four anatomical communities [7,8]. We pay attention to the cluster formation in the weak and the strong synchronisation regimes.

In the weak synchronisation regime, the four dynamical clusters C closely coincide with the functional subdivision (anatomical communities) of the cortex – C_1 (V), C_2 (A), C_3 (SM), C_4 (FL) (figure 4). However, a few nodes bridge different anatomical communities and dynamical clusters. These areas sit in one anatomical community but are involved in multimodal associations with areas in other communities [7]. For example, the area $I = 14$ (anatomically named as ‘7’ in the cat cortex and belonging to the visual system) appears in the dynamical cluster C_3 , mainly made up of somato-motor areas (figure 4 (C_3)).

In the synchronisation regime typical for strong coupling ($g \gtrsim 0.09$), the mean field signals of the areas are highly correlated. The system dynamics are mainly characterised by two dominant clusters that contain the majority of nodes and with a few single areas as separate clusters (figure 5). These dynamical clusters corresponding to the major parts of the V, SM and FL communities (in weak regime as C_1, C_3, C_4) merge into a single large cluster containing most of the nodes of the network (figure 5 (C_3)). Thus, the SM community plays a crucial role in the formation of this large dynamical cluster because of its strong intercommunity connections to the other communities. However, the auditory system A remains separate (figure 5 (C_2)). There are also two single areas acting independently and

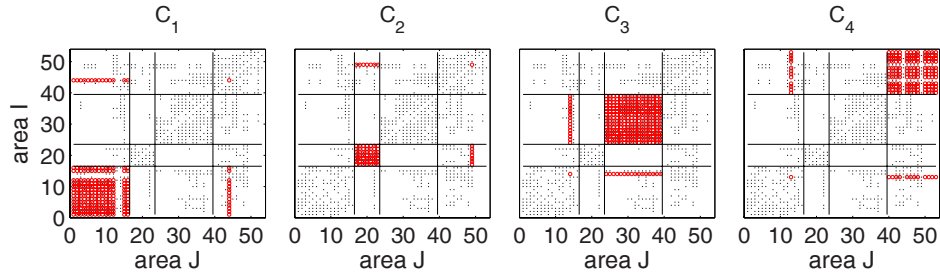


Figure 4. Dynamical clusters present in weak coupling regime ($g = 0.07$).

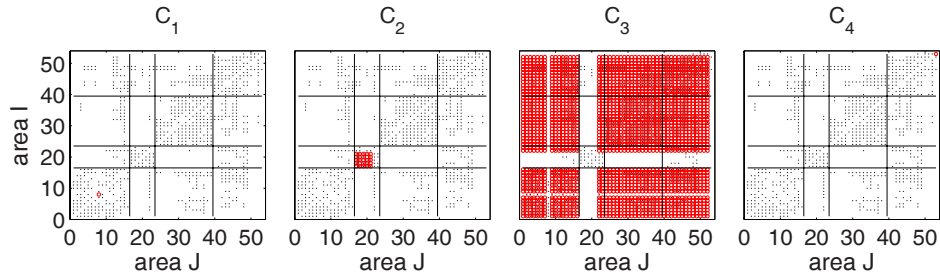


Figure 5. Dynamical clusters present in strong synchronisation regime at $g = 0.12$.

having minimal intensities – area $I = 8$ from V system ($S_8 = 11$) and area $I = 53$ from FL ($S_{53} = 8$), as C_1 and C_4 clusters.

The independent areas in the strong coupling regime as well as the bridging nodes in the weak coupling regime may vary for different parameter combinations.

5. Functional networks

Focusing on the biologically relevant weak coupling regime, we extract a *functional network* M^F [4] by applying a threshold r_{th} to the correlation r . If $r(I, J) \geq r_{th}$ a pair of areas is considered to be functionally connected ($M^F(I, J) = 1$). The functional networks M^F at different r_{th} are compared to the topological structures of the anatomical network M^C and we examine how the various levels of synchronisation reveal different scales in the network topology. Typical patterns of functional connectivity are shown in figure 6.

The dynamics of the system display a hierarchical organisation. Starting with r_{th} close to the maximal value of r , functional connections are established only between a few areas with reciprocal links, e.g., at $r_{th} = 0.07$, about $2/3$ of areas are expressed, connected only with 10% of the reciprocal links (figure 6a). Within each anatomical community V, A, SM and FL, a core subnetwork is functionally manifested in the form of connected components without intercommunity connections. At lower r_{th} , the components grow and merge, as more areas from the communities

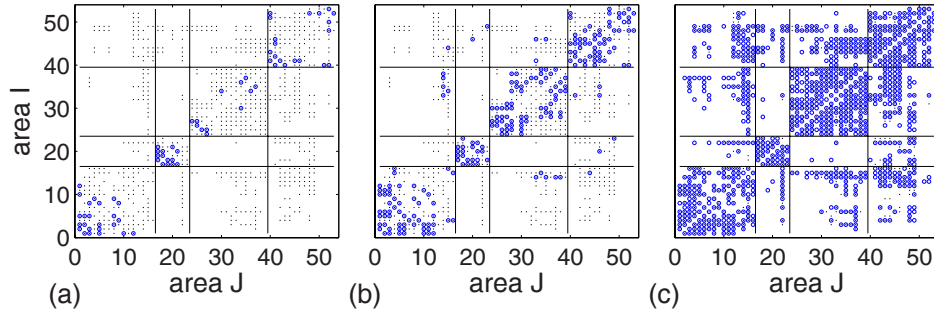


Figure 6. Functional networks extracted for $g = 0.07$ at various thresholds: (a) $r_{th} = 0.070$, (b) $r_{th} = 0.055$, (c) $r_{th} = 0.019$. The small dots indicate the anatomical connections.

appear in the functional network, together with a few intercommunity connections (figure 6b). We assume that the core subnetwork within each community performs specialised functions. About 1/3 of the anatomical reciprocal links and very few unidirectional links are already enough to link all of the cortical areas into a single, connected functional network (figure 6b). M^F with such a low connection density already resembles the main properties of M^C : high clustering and community structure. The M^C is still much denser than M^F , suggesting high robustness and the existence of many parallel paths of information processing in the brain. At $r_{th} = 0.019$ (figure 6c), all bidirectional links and about 70% of unidirectional links are present. The functional connectivity closely reflects the anatomical network.

6. Role of node intensity in the dynamics of the system

Further, the activity of the areas, expressed in the form of the mean firing rate (MFR) was registered during the simulations. The firing frequency of an area is calculated by averaging the number of spikes of neurons over the time of simulation and the number of neurons in the area. The neuronal activity is mainly determined by the structural properties of the network like intensity S of the nodes (S is the sum of strengths of incoming links to the node) and by the coupling strength between the areas.

We focus on the firing dynamics of areas in the weak synchronisation regime (figure 7a). Due to the diffusive homogeneous electrical coupling, the neurons continuously influence each other. Many of them are most of the time silent and such low level of activity acts as a dumping on the others. The higher the intensity of an area, the lower the firing frequency (figure 7b).

For a comparison, we show the firing rate when the neurons are modelled by a Morris–Lecar model coupled with *chemical synapses* (see details of the model in [14]). The main curve profile remains unchanged for different values of internal and external coupling (figure 8a). Modification of the inhibitory ($g_{1,inh}$) coupling shows a shift of the curve in the vertical direction, i.e., lower frequencies are achieved by higher inhibition. This fact is used in suppression of the redundant synchronisation in epilepsy [13].

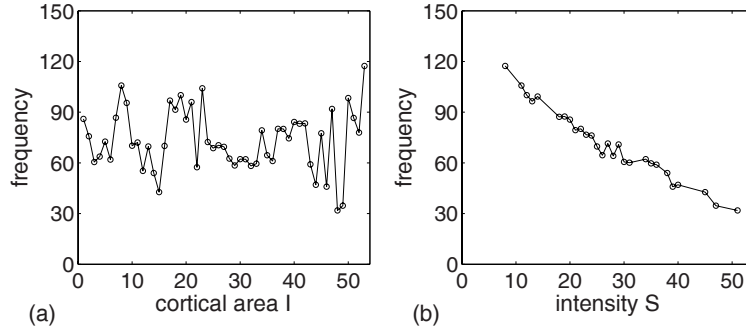


Figure 7. FHN model at coupling values $g = 0.07$. (a) Firing frequency of cortical areas. (b) Dependence of the average firing frequency on the intensity of the area.

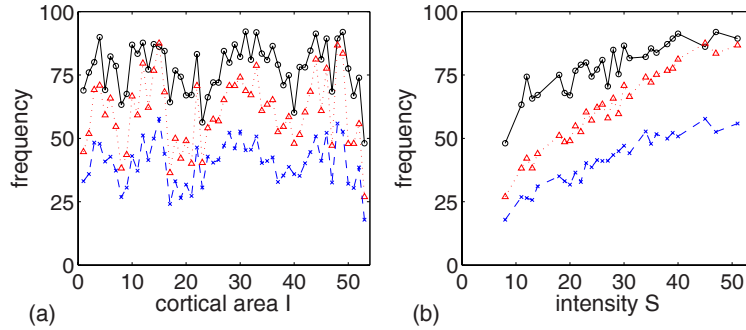


Figure 8. (a) Dependence of the firing rate on coupling strength. Here, we distinguish: $g_{2,exc}$ (inter-area excitatory coupling strength) and $g_{1,inh}$ (intra-area inhibitory coupling strength). $g_{2,exc} = 0.15$ in all cases. Solid line: $g_{1,inh} = 0.15$; dotted: $g_{1,inh} = 0.25$; dashed: $g_{1,inh} = 0.4$. (b) Correlation between different $g_{1,inh}$ parameters and S ($g_{2,exc} = 0.25$).

Figure 8b depicts the relationship between the MFR and the intensity of node. The neuron receives a signal in the form of pulses from neighbouring neurons and from remote areas. This occasional, highly stimulating input triggers further neural activity. The more input a neuron or a cortical area receives, the more often it or its neurons will fire. Thus, the higher the intensity of an area, the higher the firing frequency.

We try to find a simple analytical solution to explain the observed firing rates. A simple approach commonly used to simulate activity of neural networks is to define an activity function describing the average response of the neurons to the input from its neighbours. In a general form the equations are

$$r_i(t + 1) = F(h_i), \tag{4}$$

where

$$h_i = \sum_{j=1}^N W_{ij} r_j(t) + I, \quad i = 1, \dots, N. \quad (5)$$

r_i represents the average firing rate of the neurons in an area and $F(h_i)$ is a sigmoidal function normalised to $[0, 1]$. W_{ij} is the weighted adjacency matrix of the cortical network, and I represents the activation induced by external noise perturbations. Such a function sums up all inputs the neurons in an area receive and returns a normalised output resembling its average activity response.

Several studies have already employed this simple scheme for modelling of the cat cortical network [6]. The mean activity level of a cortical area (in our case equivalent to MFR) strongly depends on the amount of input received from its neighbours. The more input an area receives, the more neurons will fire. In the weak coupling regime we can assume a linear approximation of $F(h_i)$:

$$F(h_i) = ah_i. \quad (6)$$

With this approximation, at the steady state $r_i(t+1) = r_i(t)$ we have

$$r_i = a \left(\sum_j^N W_{ij} r_j + I \right). \quad (7)$$

We can show that the firing rates in figure 8 for various coupling strengths can be well fitted by the results from eq. (7) with suitable parameters a and I . More details can be found in [14].

7. Conclusions

We have investigated the relationship between topological structures and synchronisation dynamics of neural networks using a network of cat corticocortical connectivity. The simulated model system, a network of networks, represents a multilevel model. The study focuses on the role of structural organisation of the dynamical clustering, by modelling each cortical area by a one-level SW subnetwork. The main finding is that in a biologically plausible regime of weak synchronisation the dynamics of such multilevel model show a hierarchical organisation that reveals different levels of modular organisation in the anatomical connectivity of the corticocortical networks. Several areas important for intercommunity communication and information integration act as bridges between different anatomical communities and functional clusters. Large coupling leads to a strong synchronisation of areal activity with similar dynamical behaviour as observed, e.g., in epileptic seizures.

The role of intensity is discussed in relation to the firing rate of individual areas. In the weak coupling regime, a hierarchical model of FitzHugh–Nagumo neurons with diffusive coupling shows that the frequency of firing is anti-correlated to the areal intensity. Such behaviour is in contrast to the dynamics of the system simulated with Morris–Lecar neurons coupled with more common chemical synapses. In this case the average firing frequency of neurons in one area reflects the strength of

the areal connectivity to the other areas. The higher the areal intensity, the higher the firing frequency. The analysis of the firing rate with a simple model of network activity (eqs (4)–(7)) confirms the dependence of the firing rate on the intensity as we have observed in the model with chemical coupling.

The presented analysis of the dynamical clusters provides a meaningful bridge that mediates the gap between the topology (communities) and function (functional subdivision) of the brain cortex. A carefully extended model (more complex dynamics of neuron and structure of subnetworks) could capture more realistic information processing in the brain in the future.

Acknowledgements

This work was supported by Helmholtz Institute (HI) for Mind and Brain Dynamics, HI for Supercomputational Physics, Program ‘Familiengerechte Hochschule/Chancengleichheit’, BIOSIM - The Network of Excellence and DFG Forschergruppe ‘Computational Modeling of Behavioral, Cognitive and Neural Dynamics’.

References

- [1] D J Watts and S H Strogatz, *Nature (London)* **393**, 440 (1998)
A-L Barabási and R Albert, *Science* **286**, 509 (1999)
S Boccaletti, V Latora, Y Moreno, M Chavez and D-U Hwang, *Phys. Rep.* **424**, 175 (2006)
- [2] A Arenas, A Díaz-Guilera and C J Pérez-Vicente, *Phys. Rev. Lett.* **96**, 114102 (2006)
C S Zhou, A E Motter and J Kurths, *Phys. Rev. Lett.* **96**, 034101 (2006)
- [3] O Sporns, D R Chialvo, M Kaiser and C C Hilgetag, *Trends Cogn. Sci.* **8**, 418 (2004)
O Sporns, G Tononi and G M Edelman, *Behav. Brain. Res.* **135**, 69 (2002)
D S Bassett and E Bullmore, *Neuroscientist* **12(6)**, 512 (2006)
- [4] V M Eguíluz, D R Chialvo, G Cecchi, M Baliki and A V Apkarian, *Phys. Rev. Lett.* **94**, 018102 (2005)
C J Stam, B F Jones, G Nolte, M Breakpear and P Scheltens, *Cereb. Cortex* **26(1)**, 63 (2006)
- [5] F H Lopes da Silva, A Hoeks, H Smits and L H Zetterberg, *Kybernetik* **15**, 27 (1974)
F Wendling, J J Bellanger, F Bartolomei and P Chauvel, *Biol. Cybern.* **83**, 367 (2000)
C J Honey, R Kötter, M Breakpear and O Sporns, *Proc. Natl. Acad. Sci.* **104(24)**, 10240 (2007)
- [6] R Kötter and F T Sommer, *Philos. Trans. R. Soc. London* **B355**, 127 (2000)
M P Young, C C Hilgetag and J W Scannell, *Philos. Trans. R. Soc. London* **B355**, 147 (2000)
- [7] J W Scannell, G A P C Burns, C C Hilgetag, M A O’Neill and M P Young, *Cereb. Cortex* **9**, 277 (1999)
- [8] C C Hilgetag, G A Burns, M A O’Neill, J W Scannell and M P Young, *Philos. Trans. R. Soc. London* **B355**, 91 (2000)
- [9] A S Pikovsky and J Kurths, *Phys. Rev. Lett.* **78(5)**, 775 (1997)
- [10] M P Young, *Spatial Vis.* **13**, 137 (2000)

- [11] L Zemanová, C S Zhou and J Kurths, *Physica* **D224**, 202 (2006)
C S Zhou, L Zemanová, G Zamora, C C Hilgetag and J Kurths, *Phys. Rev. Lett.* **97**, 238103 (2006)
C S Zhou, L Zemanová, G Zamora-López, C C Hilgetag and J Kurths, *New J. Phys.* **9**, 178 (2007)
- [12] E Niedermeyer and F Lopes da Silva, *Electroencephalography: Basic principles, clinical applications, and related fields* (Williams & Wilkins, 1993)
- [13] P Kudela, P J Franaszczuk and G K Bergey, *Biol. Cybern.* **88**, 276 (2003)
- [14] M Barbosa, K Dockendorf, M Escalona, B Ibarz, A Miliotis, I Sendiña-Nadal, G Zamora and L Zemanová, Parallel computation of large neuronal networks with structured connectivity, in *Lectures in supercomputational neuroscience: Dynamics in complex brain networks* edited by P Beim Graben, C S Zhou, M Thiel and J Kurths (Springer, Berlin, 2007)